

PACS numbers: 42.55.Px; 07.57.Hm; 42.65.Re
DOI: 10.1070/QE2008v038n10ABEH013590

Amplification of mid- and far-IR pulses in synchronously pumped low-dimensional heterostructures

V.A. Kukushkin

***Abstract*. The synchronous propagation of optical pulses and mid- and far-IR pulses in waveguide low-dimensional quantum-well semiconductor heterostructures is considered. It is shown that low-frequency radiation can be considerably amplified in these systems even at room temperature because a high-power high-frequency pulse produces transient population inversion at the corresponding low-frequency transition formed by the dimensional quantisation levels of the semiconductor. The optimal parameters of the pump optical pulse and heterostructure are determined at which mid- or far-IR picosecond pulses of power $\sim$100 mW or 0.1 mW, respectively, can be amplified by more than two orders of magnitude without considerable changes in their duration and shape.**

Keywords: *quantum wells, intersubband transitions, synchronous pumping, amplification of IR radiation.*

1. Introduction

The development of sources of high-power short pulses in the mid- and far-IR ranges is one of the priority directions in modern quantum electronics. Such sources are required both for fundamental studies, for example, investigations of surface plasmon–polariton waves and coherent control of intersubband transitions in semiconductor nanostructures and for numerous applications such as nondestructive probing of weakly conducting materials and biological tissues, electromagnetic therapy, spectroscopy of organic molecules, modulation of optical radiation at terahertz frequencies, etc. Among numerous variants of such devices, low-dimensional semiconductor heterostructures – quantum wells (QWs), quantum wires, and quantum dots, are the most efficient and convenient for practical applications. This is explained by the simplicity of varying the frequency of transitions between their dimensional quantisation levels (corresponding to emission wavelengths from units to hundreds of microns) and by the convenience of current pumping providing the population inversion at the laser transition.

V.A. Kukushkin Institute of Applied Physics, Russian Academy of Sciences, ul. Ul'yaniova 46, 603950 Nizhnii Novgorod, Russia; e-mail: vakuk@appl.sci-nnov.ru

Received 4 April 2007; revision received 18 June 2007
Kvantovaya Elektronika **38** (10) 909–916 (2008)
Translated by M.N. Sapozhnikov

Unfortunately, free-electron and hole absorption and the diffraction broadening of a beam lead to a strong nonresonance attenuation of the IR power in such devices, which rapidly increases with increasing wavelength. As a result, lasing can be achieved in such structures only at large enough gains required for compensating high losses. However, the production of a considerable population inversion at a low-frequency laser transition between dimensional quantisation levels lying in the same band of a semiconductor is complicated due to the short lifetime of the upper laser state, which can be comparable to or shorter than the lower-state lifetime. This problem was solved in quantum cascade lasers (QCLs) [1], where the lower level is rapidly depleted due to tunnelling of carriers from it through the energy barrier to the adjacent level or due to transitions of carriers to lower-lying levels accompanied by emission of an optical phonon. Unfortunately, such lasers are manufactured of complex heterostructures consisting of many layers with controllable parameters, which should be cooled to temperatures considerably lower than room temperature.

Nevertheless, a high enough inversion at the laser transition can be produced in the pulsed regime for times shorter than the upper-level lifetime. This time is determined by scattering of carriers by each other (at concentrations considered below, the scattering time exceeds 5 ps [2]), emission of an optical phonon ($\sim$1 ps [3]), scattering by impurities (4–5 ps for structures under study [4]) or by scattering from rough QW surfaces (for 150–250-Å-thick QWs considered below, the scattering time lies in the range from 4 to 50 ps [5] and, being comparable with the two latter times or exceeding them, is neglected in estimates performed below). Such inversion can be achieved under the action of a high-power pump pulse on a system of electronic states formed by dimensional quantisation levels appearing in a QW. The pump pulse equalises the population of subbands in the valence and conduction bands of a semiconductor, thereby producing inversion at the intraband IR laser transition in the conduction band. As a result, it becomes possible to amplify an IR pulse at the corresponding frequency, which propagates together with the pump pulse and has approximately the same duration. As will be shown below, this effect can be obtained in much simpler heterostructures than those used in QCLs without cooling them below room temperature. In addition, unlike QCLs in these heterostructures, free carriers are located only in QWs, which considerably reduces nonresonance losses of IR radiation, thereby enhancing the lasing efficiency.

Note here that the laser transition inversion by high-power pump pulses of duration shorter than the upper-level

lifetime was performed in synchronously pumped dye lasers [6], colour centres in alkali halide crystals [7], and optical fibres [8] (see also the review of these and other papers on synchronously pumped lasers in [9]). The application of this method for low-dimensional semiconductor heterostructures is complicated by the specific structure of their dimensional quantisation levels, which is manifested, in particular, in a comparatively small inhomogeneous broadening of the laser transition and a large inhomogeneous broadening of the pump absorption band (see below). As a result, pumping populates both the upper and lower laser states, which can reduce the gain below the loss level, thereby making amplification impossible. However, as shown in the present paper, parameters can be selected so that absorption of an IR pulse at the laser transition due to this effect will be nonresonance and therefore suppressed.

Of course, to realise the method proposed, it is necessary to find the optimal parameters of the optical pump pulse and heterostructure depending on the wavelength of the IR pulse being amplified. This is the subject of this paper.

2. Amplification of an IR signal in waveguide heterostructures with QWs pumped by an optical pulse

To convert optical pulses to IR pulses by using the given scheme, a waveguide structure providing the transverse confinement of their fields and having a small absorption coefficient at both wavelengths is required. A single-plasmon waveguide, which is successfully used in mid- and far-IR QCLs [10, 11] and is modified for supporting the optical mode at the wavelength $\lambda_1 \simeq 0.8$ μm [12], can play the role of such a structure (Fig. 1). Let us denote the electromagnetic fields of the optical and IR pulses propagating in it by $\boldsymbol{E}_1$, $\boldsymbol{B}_1$, and $\boldsymbol{E}_2$, $\boldsymbol{B}_2$, respectively. They can be expressed in terms of the complex amplitudes $\tilde{\boldsymbol{E}}_n$, $\tilde{\boldsymbol{B}}_n$ $(n = 1, 2)$ in the form

$$\boldsymbol{E}_n,\ \boldsymbol{B}_n \equiv \frac{1}{2}\tilde{\boldsymbol{E}}_n,\ \tilde{\boldsymbol{B}}_n \exp(-\mathrm{i}\omega_n t) + \text{c.c.} \tag{1}$$

By neglecting the radiation mode field, which is emitted outside the waveguide (and is much smaller than the field of guided modes), we can expand the complex amplitudes of both fields in guided modes $\boldsymbol{e}_{nlk} \equiv \tilde{\boldsymbol{e}}_{nlk}(y, z)\exp(\mathrm{i}kx)$, $\boldsymbol{b}_{nlk} \equiv \tilde{\boldsymbol{b}}_{nlk}(y, z)\exp(\mathrm{i}kx)$ [13]

$$\tilde{\boldsymbol{E}}_n = \sum_{lk} \mathcal{E}_{nlk}\boldsymbol{e}_{nlk}, \tag{2}$$

$$\tilde{\boldsymbol{B}}_n = \sum_{lk} \mathcal{E}_{nlk}\boldsymbol{b}_{nlk}, \tag{3}$$

where the subscript l denotes the polarisation of a mode ($l = 1$ for the TE mode and $l = 2$ for the TM mode) and the subscript k (which is, in general, a multifunction of n and l) is the wave index of the mode along the direction x. By using the standard theory of waveguide excitation [13], the values of $\mathcal{E}_{nlk}$ can be found from equations

$$\mathrm{d}\mathcal{E}_{nlk}/\mathrm{d}x = \int \tilde{\boldsymbol{j}}_n \boldsymbol{e}_{nl-k}\mathrm{d}S/N_{nlk}, \tag{4}$$

where $\tilde{\boldsymbol{j}}_n \equiv -\mathrm{i}\omega_n\tilde{\boldsymbol{P}}_n$ are the complex amplitudes of current densities, which are expressed in terms of the complex amplitudes of corresponding polarisations $\tilde{\boldsymbol{P}}_n$ produced at

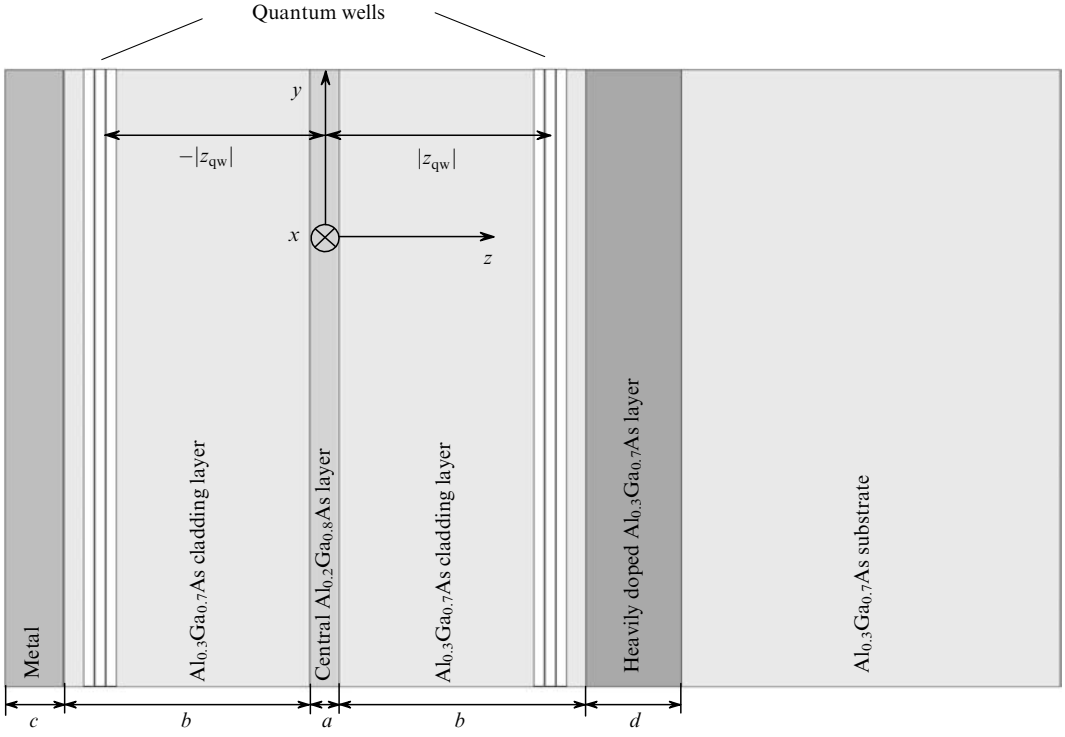

Figure 1. Scheme of a stripe waveguide QW heterostructure consisting of the $Al_{0.2}Ga_{0.8}As$ core and the external cladding formed by two $Al_{0.3}Ga_{0.7}As$ layers ($\varepsilon_{Al_{0.2}Ga_{0.8}As} > \varepsilon_{Al_{0.3}Ga_{0.7}As}$) (dielectric waveguide), a surface metal coating, and a heavily doped $Al_{0.3}Ga_{0.7}As$ layer (single-plasmon waveguide), a weakly conducting $Al_{0.3}Ga_{0.7}As$ substrate, and two QW layers responsible for the conversion of the optical pulse to the IR pulse ($c \sim 10 - 100$ nm, $d \sim 2$ μm; the optimal values of parameters a, b, and $|z_{qw}|$ are found in section 3).

the optical and IR transitions; $dS \equiv dydz$; expressions for $\boldsymbol{e}_{nl-k}$ are presented in [13]; N_{nlk} is the norm of the mode with indices nlk (according to the definition in [13], $N_{nlk} < 0$). We will analyse Eqn (4) for a typical waveguide with the transverse size along y not exceeding ~ 10 μm (Fig. 1). For such parameters for an optical field with $\lambda_1 \simeq 0.8$ μm, only one variation along y is possible, and guided modes can be approximately described within the framework of the theory of an infinitely broad (along the y axis) stripe waveguide [13] according to which $\tilde{\boldsymbol{e}}_{nlk}$ and $\tilde{\boldsymbol{b}}_{nlk}$ are the functions of only z. According to estimates (see section 3), the optimal thickness of the central layer is small enough, so that the waveguide will support the propagation of only two transverse optical TE and TM modes. We will consider below a typical situation for QW heterolasers, when the fields $\boldsymbol{E}_1$ and $\boldsymbol{E}_2$ are formed by the TE and TM modes, respectively, so that $l = 1$ and $k = k_1$ for the optical field, while for IR radiation, we have $l = 2$ and $k = k_2$, and, therefore, indices can be omitted below.

To solve Eqn (4), it is necessary to express $\tilde{\boldsymbol{j}}_n \equiv -i\omega_n \tilde{\boldsymbol{P}}_n$ in terms of $\mathcal{E}_n$. This can be done by considering the dynamics of carriers in QWs produced, for example, in the $Al_xGa_{1-x}As$ system (Fig. 2). For the aims of the present work, it is sufficient to consider only four subbands in each QW: in the valence band – one subband (0) of heavy or light holes (the criterion for selection of this subband is presented below) and the highest-lying subband (1) of heavy holes; and in the conduction band – the two lowest-lying electron subbands (2 and 3), which form the laser transition for amplification of IR radiation (Fig. 2). In this case, other low-frequency transitions present in the heterostructure can be neglected because their frequencies considerably differ from the carrier IR frequency, which is resonant with the $3 \to 2$ transition frequency. Interband transitions in such a scheme correspond to wavelengths $\lambda \sim 0.7 - 0.8$ μm, whereas the intersubband $3 \to 2$ transition lies in the region above 10 μm[*]. It is well known that all the five transitions ($2 \to 1$, $3 \to 2$, $3 \to 1$, $2 \to 0$, and $3 \to 0$) for asymmetric QWs with different heights of the left and right barriers considered here are allowed dipole transitions and have

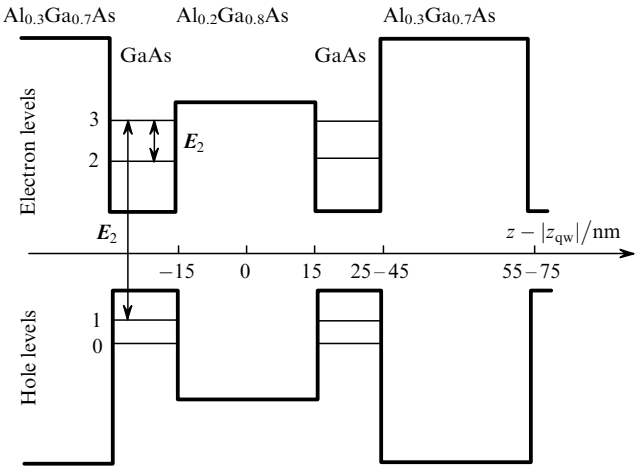

Figure 2. Scheme of electron (hole) dimensional quantisation levels in a QW in which a weak IR pulse $\boldsymbol{E}_2$ is amplified due to the conversion of a simultaneously propagating strong optical pulse $\boldsymbol{E}_1$. Each of the levels is a subband of electronic states with different projections of quasi-momenta p_x and p_y on the QW plane.

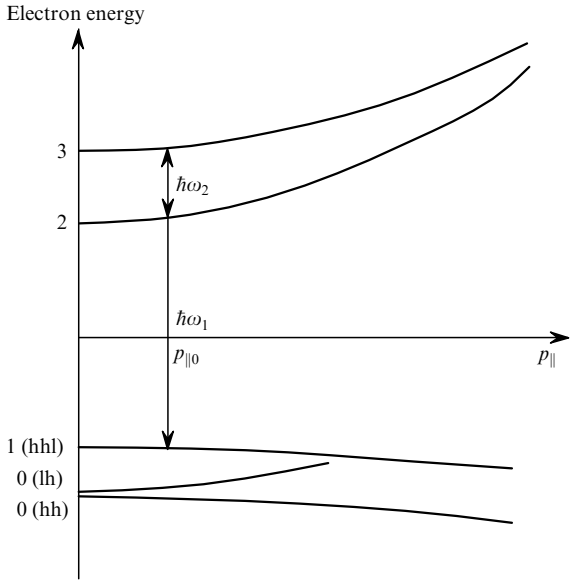

Figure 3. Scheme of the band structure of GaAs near the Γ point with QWs grown in the $\langle 001 \rangle$ direction ($p_\parallel \equiv (p_x^2 + p_y^2)^{1/2}$). Energy is measured from the middle of the gap; 0 is the subband of the light (lh) or heavy (hh) holes; 1 is the highest-lying subband of heavy holes (hh1); 2 and 3 are the lowest-lying electron subbands.

large nondiagonal matrix elements of the order of 0.3 – 1 nm for interband transitions and 1 – 3 nm for intersubband transitions [15].

We will assume that the electron energy $\tilde{e}_i$ in each subband ($i = 0, 1, 2, 3$) depends only on their quasi-momentum $p_\parallel \equiv (p_x^2 + p_y^2)^{1/2}$ in the QW plane (isotropic approximation [16, 17]), so that $\tilde{e}_i = \tilde{e}_{i0} + p_\parallel^2/(2m_i)$, where $\tilde{e}_{i0}$ is the energy of electrons with zero $p_\parallel$ and m_i is the effective mass (Fig. 3). Let $p_{\parallel 0}$ be the value of $p_\parallel$ at which the $3 \to 1$ transition frequency [i.e. the value $(\tilde{e}_3 - \tilde{e}_1)/\hbar$] coincides with the frequency ω_1. By denoting the deviation of the $3 \to 1$ transition frequency from ω_1 by Δ, we see that $p_\parallel$ is uniquely expressed in terms of $\Delta \equiv (p_\parallel^2 - p_{\parallel 0}^2) \times [1/(2m_3) + 1/(2m_1)]/\hbar$, the value of Δ completely characterising the inhomogeneous broadening in the given system and determining the deviation of frequencies of all other transitions in the four-level system from their values for $p_\parallel = p_{\parallel 0}$. A simple calculation shows that the number of electronic states (per unit volume) with different p_x and p_y for which the $3 \to 1$ transition frequency lies in the interval from $\omega_1 + \Delta$ to $\omega_1 + \Delta + d\Delta$ is equal to $N d\Delta$, where

$$N \simeq m_1 m_3/[2\pi\hbar(m_1 + m_3)\Delta z_{qw}] \tag{5}$$

is the corresponding density of states; $m_1 \simeq 0.5m$; $m_3 \simeq 0.07m$ [17, 18]; m is the free electron mass; and Δz_{qw} is the QW width. By assuming that ω_2 is equal to the $3 \to 2$ transition frequency for $\Delta = 0$, elementary calculations show that the deviation of the $3 \to 2$ transition frequency from ω_2 is $-\eta\Delta$, where

$$\eta = m_1(m_3 - m_2)/[m_2(m_1 + m_3)] \lesssim 0.1, \tag{6}$$

[*] Of course, the further consideration can be easily applied to the case when the laser transition is formed by the hole subbands rather than by the electron subbands [14] and corresponds to wavelengths above 70 μm [15].

and η is estimated by using simple analytic expressions for effective electron masses m_2 and m_3 in an infinitely deep QW of width exceeding 150 Å [18]. Note here that, as in QCLs [1], $\eta > 0$ and $\eta \ll 1$ due to the larger effective electron mass in subband 3 compared to subband 2. Thus, the inhomogeneous broadening of the $3 \to 2$ transition is considerably smaller than that of the $3 \to 1$ transition.

Now we can determine the criterion for the choice of the subband of light or heavy holes (denoted above by 0). It follows from Fig. 3 and the consideration performed above that the optical field populates subband 2 for $p_\parallel$ lying where ω_1 is resonant with transitions between subbands 2 and 1 or hole subbands lying below subband 1.This leads, of course, to absorption of the IR field at the $3 \to 2$ transition in this region of $p_\parallel$ (or, equivalently, Δ) and is undesirable. However, as follows from the previous consideration, the $3 \to 2$ transition frequency decreases with increasing Δ due to the nonzero coefficient η, thereby detuning from the resonance with the IR field. As a result, this detuning for the specified Δ can exceed the homogeneous width of the $3 \to 2$ transition line, calculated taking into account the field of a strong optical pulse (which, as follows from estimates with the use of optimal parameters for the IR field amplification found in the next section, does takes place), and absorption of IR radiation at this transition can be suppressed. It is obvious that the hole subband (denoted above by 0) for which the specified value of Δ (and, therefore, the corresponding change $-\eta\Delta$ in the $3 \to 2$ transition frequency) is minimal will make the greatest contribution to absorption of the IR field. A simple analysis based on results obtained in [18] shows that the minimum value is $\Delta = (0.3 \div 1)\omega_2$.

As a result, each QW can be described by a four-level scheme with the density matrix ρ_{ij} depending only on Δ. The nondiagonal elements of the matrix can be represented as the products of rapidly varying exponential factors with the corresponding resonance frequencies $\omega_{1,2}$ (for interband and intersubband transitions, respectively) and of slowly varying amplitudes $\tilde{\rho}_{ij}$. The latter can be found from the system of equations [19]

$$
\begin{aligned}
&\mathrm{d}\tilde{\rho}_{21}/\mathrm{d}t + \Gamma_{21}\tilde{\rho}_{21} = -\mathrm{i}e_1\tilde{\rho}_{32}^* + \mathrm{i}e_2^*\tilde{\rho}_{31},\\
&\mathrm{d}\tilde{\rho}_{31}/\mathrm{d}t + \Gamma_{31}\tilde{\rho}_{31} = \mathrm{i}e_1 n_{13} + \mathrm{i}e_2\tilde{\rho}_{21},\\
&\mathrm{d}\tilde{\rho}_{20}/\mathrm{d}t + \Gamma_{20}\tilde{\rho}_{20} = \mathrm{i}e_1 n_{02} + \mathrm{i}e_2^*\tilde{\rho}_{30},\\
&\mathrm{d}\tilde{\rho}_{30}/\mathrm{d}t + \Gamma_{30}\tilde{\rho}_{30} = -\mathrm{i}e_1\tilde{\rho}_{32} + \mathrm{i}e_2\tilde{\rho}_{20},\\
&\mathrm{d}\tilde{\rho}_{32}/\mathrm{d}t + \Gamma_{32}\tilde{\rho}_{32} = \mathrm{i}e_2 n_{23} + \mathrm{i}e_1\tilde{\rho}_{21}^* - \mathrm{i}e_1^*\tilde{\rho}_{30},
\end{aligned}
\tag{7}
$$

where

$$
\Gamma_{21} = \Gamma_{31} = \gamma + \mathrm{i}\Delta;\ \Gamma_{20} = \Gamma_{30} = \gamma + \mathrm{i}[\Delta - (0.3 \div 1)\omega_2];
$$

$$
\Gamma_{32} = \gamma - \mathrm{i}\eta\Delta; \tag{8}
$$

$n_{ij} = \rho_{ii} - \rho_{jj}$ is the population differences; $e_1 \equiv \mathcal{E}_1 \boldsymbol{d}_{\mathrm{opt}}\boldsymbol{e}_1/(2\hbar)$ and $e_2 \equiv \mathcal{E}_2\boldsymbol{d}_{\mathrm{IR}}\boldsymbol{e}_2/(2\hbar)$ are the Rabi frequencies for optical and IR fields, respectively; $\boldsymbol{d}_{31} \simeq \boldsymbol{d}_{20} \equiv \boldsymbol{d}_{\mathrm{opt}}$ and $\boldsymbol{d}_{32} \equiv \boldsymbol{d}_{\mathrm{IR}}$ are the dipole moments for interband and intersubband transitions; to simplify expressions derived below, it is assumed that the rates of polarisation relaxation at all the transitions between levels 0, 1, 2, and 3 are the same and equal to γ, i.e. $\gamma_{21} = \gamma_{31} = \gamma_{20} = \gamma_{30} = \gamma_{32} \equiv \gamma$.

Because the durations of optical and IR pulses exceed the relaxation time $\sim 1/\gamma$ (or are at least comparable with it, see section 3), it is sufficient to obtain the stationary solution of system (7) for estimates. Assuming that the IR pulse field is much weaker than the optical field, we can use the perturbation theory in a small parameter $|\mathcal{E}_2|/|\mathcal{E}_1| \ll 1$, by retaining only terms of the zero and first orders in $\mathcal{E}_2$. This gives

$$
\tilde{\rho}_{31} = \mathrm{i}e_1 n_{13}/\Gamma_{31}, \tag{9}
$$

$$
\tilde{\rho}_{20} = \mathrm{i}e_1 n_{02}/\Gamma_{20}, \tag{10}
$$

$$
\tilde{\rho}_{32} = \mathrm{i}e_2\frac{n_{23} - n_{13}|e_1|^2/(\Gamma_{31}^*\Gamma_{21}^*) + n_{02}|e_1|^2/(\Gamma_{20}\Gamma_{30})}{\Gamma_{32} + |e_1|^2/\Gamma_{21}^* + |e_1|^2/\Gamma_{30}}. \tag{11}
$$

The population differences entering (10) and (11) can be determined from equations [19]

$$
\mathrm{d}n_{13}/\mathrm{d}t + r(n_{13} - \bar{n}_{13}) = -4\mathrm{Im}(e_1^*\tilde{\rho}_{31}) - 2\mathrm{Im}(e_2^*\tilde{\rho}_{32}), \tag{12}
$$

$$
\mathrm{d}n_{02}/\mathrm{d}t + r(n_{02} - \bar{n}_{02}) = -4\mathrm{Im}(e_1^*\tilde{\rho}_{20}) + 2\mathrm{Im}(e_2^*\tilde{\rho}_{32}), \tag{13}
$$

$$
\mathrm{d}n_{23}\mathrm{d}t + r(n_{23} - \bar{n}_{23}) = -2\mathrm{Im}(e_1^*\tilde{\rho}_{31}) + 2\mathrm{Im}(e_1^*\tilde{\rho}_{20}) - 4\mathrm{Im}(e_2^*\tilde{\rho}_{32}). \tag{14}
$$

Because we consider below only the time intervals that are much shorter than the time of nonradiative $3 \to 2$ electronic transitions (and considerably shorter than the time of spontaneous radiative electronic transitions from the levels 3 and 2 to the valence band), the relaxation terms in Eqns (12)–(14) take into account only intrasubband relaxation processes with the rate r, which is assumed the same for all the subbands and considerably exceeds the rate of intersubband processes [20]. In this case, the quantities $\bar{n}_{ij} \equiv \bar{\rho}_{ii} - \bar{\rho}_{jj}$ ($i = 0, 1, 2, 3$) are quasi-equilibrium population differences determined by quasi-equilibrium Fermi electron distributions $\bar{\rho}_{jj}$. The latter, being the functions of the total numbers of electrons in subbands (during the pump pulse, these numbers increase in subbands 3 and 2 and decrease in subbands 0 and 1), slowly vary in time (at the scale $1/r$). However, according to [2], due to a rather high density of electronic states in QWs, the functions $1 - \bar{\rho}_{00}$, $1 - \bar{\rho}_{11}$, as well as $\bar{\rho}_{22}$ and $\bar{\rho}_{33}$ become comparable with unity only at the surface concentrations of excited electrons in subband 3 or 2 (or holes in subband 1 or 0) above 2×10^{11} cm^{-2}. As shown in section 3, the optimal value of this parameter for amplification of the IR pulse (even at the pump pulse end) is considerably smaller than the values presented above. Therefore, we can set $\bar{n}_{13} \simeq \bar{n}_{02} \simeq 1$ and $\bar{n}_{23} \simeq 0$ in (12)–(14). As a result, in the time $\sim 1/r$, which is considerably shorter than the duration of the pump and IR pulses (see section 3), the solutions of Eqns (12)–(14) become almost stationary until the end of pulses.

To find these solutions by using the perturbation theory with a small parameter $|\mathcal{E}_2|/|\mathcal{E}_1| \ll 1$, we should take into

account that, according to (11), the term $\mathrm{Im}(e_2^*\tilde{\rho}_{32})$ in (13) and (14) is proportional at least to $|e_2|^2$ and therefore it can be omitted in the approximation linear over e_2. As a result, the stationary solutions of Eqns (12), (13), and (14) take the form

$$n_{13} = \frac{1}{1 + 4(\gamma/r)|e_1|^2/(\gamma^2 + \Delta^2)}, \tag{15}$$

$$n_{02} = \frac{1}{1 + 4(\gamma/r)|e_1|^2/\{\gamma^2 + [\Delta - (0.3 \div 1)\omega_2]^2\}}, \tag{16}$$

$$n_{23} = -\frac{2(\gamma/r)|e_1|^2}{4(\gamma/r)|e_1|^2 + \gamma^2 + \Delta^2} + \frac{2(\gamma/r)|e_1|^2}{4(\gamma/r)|e_1|^2 + \gamma^2 + [\Delta - (0.3 \div 1)\omega_2]^2} \tag{17}$$

and can be substituted into expressions (9)–(11) to obtain the explicit frequency dependences of $\tilde{\rho}_{31}$, $\tilde{\rho}_{20}$, and $\tilde{\rho}_{32}$. The dependences of $n_{23}(x = 0)$ on the dimensionless detuning are shown in Fig. 4. One can see that $n_{23} < 0$ (i.e. the $3 \to 2$ transition is inverted and the IR pulse can be amplified) for small enough $|\Delta|$, when the pump pulse efficiently populates subband 3. In this case, the maximum inversion is achieved for $\Delta = 0$ and is approximately -0.45. The opposite situation ($n_{23} > 0$, i.e. absorption of the IR pulse) takes place for large enough values of Δ in the region of $(0.3 \div 1)\omega_2$ due to the filling of subband 2 by the pump pulse. However, as mentioned above, this effect proves to be considerably suppressed due to a decrease in the $3 \to 2$ transition frequency with increasing Δ.

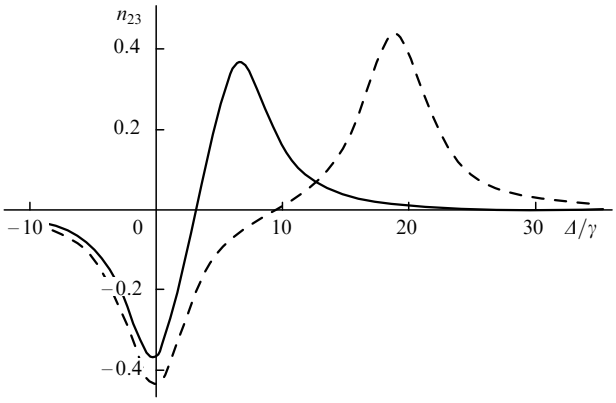

Figure 4. Dependences of $n_{23}(x = 0)$ (17) on the dimensional detuning Δ/γ for the optimal values of $2|e_1(x = 0)|/\sqrt{\gamma r} \simeq 3$ and ω_2 corresponding to $\lambda_2 = 22$ μm (solid curve, $\gamma \simeq 4 \times 10^{12}$ s^{-1}) and 60 μm (dashed curve, $\gamma \simeq 0.5 \times 10^{12}$ s^{-1}), see section 3.

The complex amplitudes of polarisations at interband and intersubband transitions can be written as

$$\tilde{\boldsymbol{P}}_1 = \boldsymbol{d}_{\mathrm{opt}} \exp(\mathrm{i}k_1 x) \int_{-\infty}^{+\infty} N(\tilde{\rho}_{31} + \tilde{\rho}_{20}) \mathrm{d}\Delta, \tag{18}$$

$$\tilde{\boldsymbol{P}}_2 = \boldsymbol{d}_{\mathrm{IR}} \exp(\mathrm{i}k_2 x) \int_{-\infty}^{+\infty} N\tilde{\rho}_{32} \mathrm{d}\Delta. \tag{19}$$

Note here that due to a small thickness of the QW, the transverse variations of optical and IR fields over the QW thickness can be neglected. As a result, the above discussion can be generalised to the case of several adjacent QWs by multiplying the right-hand sides of Eqns (18) and (19) by the total number q of QWs. According to Fig. 1, this number is equally distributed between two active regions located symmetrically with respect to the central waveguide layer.

By using Eqns (18) and (19), the definition $\tilde{\boldsymbol{j}}_n \equiv -\mathrm{i}\omega_n \tilde{\boldsymbol{P}}_n$, and Eqn (4), we can find the spatial evolution of $\mathcal{E}_n$. Thus, expression (4) for optical radiation takes the form

$$\mathrm{d}\mathcal{E}_1/\mathrm{d}x = -\alpha_1 \mathcal{E}_1 / \left(1 + |E_1/\mathcal{E}_{1\mathrm{s}}|\right)^{1/2}, \tag{20}$$

where $\mathcal{E}_{1\mathrm{s}} \equiv \sqrt{\gamma r}\,\hbar/[\boldsymbol{d}_{\mathrm{opt}} \boldsymbol{e}_1(x, z_{\mathrm{qw}})]$ is the amplitude of the field saturating interband transitions;

$$\alpha_1 \equiv -2\pi q \omega_1 N S_{\mathrm{qw}} |\boldsymbol{d}_{\mathrm{opt}} \tilde{\boldsymbol{e}}_1(z_{\mathrm{qw}})|^2/(2\hbar N_1) \tag{21}$$

is the unsaturated absorption coefficient for $\boldsymbol{E}_1$ due to the QW; S_{qw} is the QW area in the yz plane; and $z_{\mathrm{qw}} \equiv \pm|z_{\mathrm{qw}}|$ is the z coordinate of the centre of the left or right group of QWs (see Fig. 1); $\tilde{\boldsymbol{e}}_1(|z_{\mathrm{qw}}|) = -\tilde{\boldsymbol{e}}_1(-|z_{\mathrm{qw}}|)$ due to the symmetry of the optical mode. It follows for the IR field from Eqn (4) that

$$\frac{1}{\alpha_2}\frac{\mathrm{d}\ \ln|\mathcal{E}_2|}{\mathrm{d}x} = \frac{\Theta(4 + 4\sqrt{1+\Theta} + 2\Theta - \zeta\Theta)}{4\sqrt{1+\Theta}(1+\sqrt{1+\Theta})(2/\zeta - 1)} \times \left\{ \frac{1}{(1+\eta\sqrt{1+\Theta})(1+\sqrt{1+\Theta}) + \zeta\Theta/4} - \mathrm{Re}\,\frac{1}{[1 - \mathrm{i}(0.3 \div 1)\eta\omega_2/\gamma - \eta\sqrt{1+\Theta}](1+\sqrt{1+\Theta}) + \zeta\Theta/4} \right\} + \mathrm{Re}\,\frac{\mathrm{i}\Theta\zeta}{2\eta(2/\zeta - 1)(\delta_2 - \delta_1)(1 + \delta_2^2 + \Theta)} \left[1 - \mathrm{i}\delta_2 + 2(1 + i\delta_2)/\zeta\right]. \tag{22}$$

Here, $\Theta \equiv |\mathcal{E}_1/\mathcal{E}_{1\mathrm{s}}|^2$; $\zeta \equiv r/\gamma$;

$$\alpha_2 \equiv -\pi q \omega_2 (2/\zeta - 1) N S_{\mathrm{qw}} |\boldsymbol{d}_{32} \tilde{\boldsymbol{e}}_2(z_{\mathrm{qw}})|^2/(2\hbar N_2); \tag{23}$$

$$\delta_{1,2} = \frac{-\mathrm{i}(1-\eta)}{2\eta} = \pm\frac{\{-(1-\eta)^2 - 4\eta[1 - \mathrm{i}(0.3 \div 1)\eta\omega_2/\gamma + \zeta\Theta/4]\}^{1/2}}{2\eta}; \tag{24}$$

and the difference between $\tilde{\boldsymbol{e}}_2(|z_{\mathrm{qw}}|)$ and $-\tilde{\boldsymbol{e}}_2(-|z_{\mathrm{qw}}|)$ is neglected due to a large size of the IR mode. The amplification of the IR field as a function of x is described by the expression

$$\frac{|\tilde{\boldsymbol{E}}_2(x)|}{|\tilde{\boldsymbol{E}}_2(0)|} = \frac{|\mathcal{E}_2(x)|}{|\mathcal{E}_2(0)|} \exp(-x\mathrm{Im}k_2), \tag{25}$$

where the exponential factor takes into account the IR mode attenuation. The maximum value of (25) and the corresponding optimal parameters of the waveguide heter-

ostructure and optical pulse are found in the next section by analysing the numerical solution of Eqns (20) and (22).

3. Parameters of waveguide structures and optical pulses optimal for amplification of the IR signal

As pointed out above, to amplify efficiently the IR pulse, it should propagate together with the optical pulse, i.e. the group velocities of these pulses should be equal. By using data [21–23] and the standard theory of waveguides [13], we can show that for the structure presented in Fig. 1 and optical pulse with the carrier wavelength $\lambda_1 \simeq 0.8$ μm this condition is fulfilled if the central wavelength λ_2 of the IR pulse is approximately equal to 22 or 60 μm. Thus, the amplification of the IR pulse can be efficient only at these wavelengths. Nevertheless, note that it is possible, of course, to use waveguides of other designs in which the equality of the group velocities of the optical and IR modes can be achieved at other wavelengths, which provides the efficient amplification of the IR signal at a desirable wavelength.

The qualitative and numerical analysis of the waveguide structure [10–12] and equations (20) and (22) shows that the minimal losses for optical radiation and the maximum amplification of the IR pulse are achieved at $a \simeq 0.12$ μm and $b \simeq 2$ μm for $\lambda_2 = 22$ μm and at $a \simeq 0.024$ μm and $b \simeq 10$ μm for $\lambda_2 = 60$ μm (see Fig. 1). In this case, the overlap of the fields of the optical and IR pulses along the z axis in the waveguide structure is determined by the ratio of the quantity $a + 2b$ (i.e. the width of the pump-pulse distribution along the z axis) and the transverse scale of the mid- or far-IR mode (Fig. 1). By using the values of a and b presented above and data from [10–12], we find that this ratio is ~0.8 for $\lambda_2 = 22$ μm and ~0.4 for $\lambda_2 = 60$ μm.

Now it is necessary to determine the optimal values of coupling constants of QWs with the IR signal ($|\boldsymbol{d}_{32}\tilde{\boldsymbol{e}}_2(z_{qw})|$) and optical field ($|\boldsymbol{d}_{31}\tilde{\boldsymbol{e}}_1(z_{qw})|$). It is obvious from (22) and (23) that amplification of the IR field increases with increasing $|\boldsymbol{d}_{32}\tilde{\boldsymbol{e}}_2(z_{qw})|$ because $\alpha_2 \propto |\boldsymbol{d}_{32}\tilde{\boldsymbol{e}}_2(z_{qw})|^2$. As for the quantity $|\boldsymbol{d}_{31}\tilde{\boldsymbol{e}}_1(z_{qw})|$, the analysis shows that its optimum value should approximately correspond to the electron concentration $\rho_3 \equiv \int N\rho_{33}\mathrm{d}\Delta$ in subband 3 near $\Delta = 0$ at which relaxation rates $\gamma \sim r$*) due to electron–electron interaction in this subband exceed by several times the intersubband relaxation rate $1/\tau_{32}$. The higher values of $|\boldsymbol{d}_{31}\tilde{\boldsymbol{e}}_1(z_{qw})|$ correspond to higher electron concentrations in subband 3 and, therefore, to the higher values $\gamma \sim r$ (they are proportional to ρ_3 in the case under study with small occupation numbers for the states in subband 3). This in turn makes the width of the $3 \to 2$ transition line [which is equal to $\gamma + r|\mathcal{E}_1/\mathcal{E}_{1s}|^2/\{4[1 + (1 + |\mathcal{E}_1/\mathcal{E}_{1s}|^2)^{1/2}]\}$, as follows from the second term in (22)] greater than $(0.3 \div 1)\omega_2\eta$ and, therefore, causes strong absorption of the IR field at the $3 \to 2$ transition for $\Delta \simeq (0.3 \div 1)\omega_2$. On the other hand, the lower values of $|\boldsymbol{d}_{31}\tilde{\boldsymbol{e}}_1(z_{qw})|$ lead to the lower electron concentration in subband 3 and, therefore, to the lower inversion and weaker amplification of the IR field at the $3 \to 2$ transition near $\Delta = 0$.

The dependence $\gamma \sim r$ on ρ_3 can be determined by using data [2] for the relaxation rate of the $3 \to 2$ transition due to electron–electron scattering and taking into account that this rate is approximately an order of magnitude lower than the rate of intrasubband electron–electron relaxation [20]. The concentration of excited electrons near $\Delta = 0$ can be found from Eqn (17) taking into account that at time intervals shorter than the $3 \to 2$ relaxation time τ_{32}, we can set $\rho_{22} \simeq 0$ and, therefore, $\rho_{33} \simeq -n_{23}$:

$$\rho_3 = \frac{\pi N\gamma|\mathcal{E}_1/\mathcal{E}_{1s}|^2}{2(1 + |\mathcal{E}_1/\mathcal{E}_{1s}|^2)^{1/2}}. \tag{26}$$

In the case $\lambda_2 \simeq 22$ μm, the frequency ω_2 is higher than the frequency of longitudinal phonons both in GaAs and AlAs [24], so that for the optimal value of $|\boldsymbol{d}_{31}\tilde{\boldsymbol{e}}_1(z_{qw})|$ the value of τ_{32} is determined by the time of the $3 \to 2$ transition accompanied by phonon emission and is ~1 ps [3]. Thus, according to the above discussion, the optimal surface concentration of excited electrons should be close to 9.7×10^{10} cm^{-2} in a QW of width 150 Å, which, according to (26), corresponds to $|\mathcal{E}_1(0)/\mathcal{E}_{1s}(0)| \equiv 2|e_1(0)|/\sqrt{\gamma r} \simeq 3$.

If $\lambda_2 \simeq 60$ μm, then the frequency ω_2 is lower than the frequency of longitudinal optical phonons in GaAs and AlAs, so that the relaxation time of the $3 \to 2$ transition is determined by scattering from impurities and is 4–5 ps at 300 K for typical QW $Al_xGa_{1-x}As/GaAs/Al_xGa_{1-x}As$ structures [4]. Similarly to the previous case, we can easily find that the optimal concentration should be 2×10^{10} cm^{-2} for a QW of width 265 Å; together with Eqn (26), this gives the ratio $|\mathcal{E}_1(0)/\mathcal{E}_{1s}(0)| \simeq 3$.

To determine the optimal concentrations of excited electrons and parameter $|\mathcal{E}_1(0)/\mathcal{E}_{1s}(0)|$ more accurately, it is necessary to analyse the behaviour of the gain for the IR pulse (25) found by solving numerically Eqns (20) and (22). We will calculate the gain by assuming that the absorption coefficients for optical and IR fields are $\mathrm{Im}\,k_1 \simeq 0.25$ cm^{-1} [25] and $\mathrm{Im}\,k_2 \simeq 3.5$ cm^{-1} for $\lambda_2 \simeq 2$ μm [26] and $\mathrm{Im}\,k_2 \simeq 1.35$ cm^{-1} for $\lambda_2 \simeq 60$ μm [11]. The value of α_2 can be determined by setting the matrix element of the $3 \to 2$ transition equal to 3 nm [15] and estimating the norm N_2 of the IR mode by using results [11] for the wavelengths $\lambda_2 = 22$ and 60 μm. Thus, $\alpha_2 \simeq 1.47q$ and $0.086q$ (in cm^{-1}) for $\lambda_2 = 22$ and 60 μm, respectively. Such a rapid decrease of α_2 and the increase in the IR radiation wavelength is explained by the decrease in $\omega_2 \propto 1/\lambda_2$ with increasing $|N_2|$ in expression (23) for α_2.

Note that for typical values of matrix elements of interband transitions of ~0.3 nm [15], the optimal values of the parameter $|\mathcal{E}_1(0)/\mathcal{E}_{1s}(0)|$ can be achieved at comparatively small (~1 mW) peak powers of optical pulses, which are considerably lower than those obtained in experiments with mode-locked QW lasers [27]. Nevertheless, it seems advantageous to use optical pulses of input power as high as possible because the increase in $\boldsymbol{E}_1$ for the fixed ratio $|\mathcal{E}_1(0)/\mathcal{E}_{1s}(0)|$ means the decrease in $|\boldsymbol{d}_{31}\tilde{\boldsymbol{e}}_1(z_{qw})|$ and $\alpha_1 \propto |\boldsymbol{d}_{31}\tilde{\boldsymbol{e}}_1(z_{qw})|^2$ and, hence, the decrease in the absorption of the optical field, which provides more favourable conditions for its conversion to the IR signal. For the matrix elements of interband transitions of ~0.3 nm, small values of $|\boldsymbol{d}_{31}\tilde{\boldsymbol{e}}_1(z_{qw})|$ can be easily obtained by placing QW active regions into the cladding layers of a dielectric waveguide, where the optical mode decays exponentially with distance from the central layer. However, because the

*) This relation is typical for QW lasers in which the dephasing of transition dipole moments and relaxation of the distribution function of carriers are determined by the same intrasubband scattering.

inhomogeneity scale of the IR mode along the z axis considerably exceeds that for the optical field, such an arrangement of active regions by no means reduces $\alpha_2 \propto |\boldsymbol{d}_{32}\tilde{\boldsymbol{e}}_2(z_{qw})|^2$ and the gain for the IR pulse. For example, for the relaxation rates determined above and 120-W, 0.5-ps optical pulses obtained in [27], the value of $|z_{qw}|$ should be ~ 1.8 μm for the central layer of thickness 0.12 μm. For 2-ps, 60-W pulses and the 0.024-μm-thick central layer, we have $|z_{qw}| \simeq 8.5$ μm. Having these parameters, it is easy to obtain $\alpha_1 \simeq 0.075q$ (in cm^{-1}) for 120-W, 0.5-ps pulses and $\alpha_1 \simeq 0.004q$ (in cm^{-1}) for 60-W, 2-ps pulses.

When these parameters are used for numerical simulations of the behaviour of optical and IR pulses based on (20) and (22), the maximum gain for the IR signal (25) [over x and $|\mathcal{E}_1(0)/\mathcal{E}_{1s}(0)|$] exceeds unity (and, therefore, the proposed method can be used) for the number of adjacent QWs $q > 5$ for $\lambda_2 = 22$ μm and $q > 67$ for $\lambda_2 = 60$ μm.

A further increase in the number of QWs leads to a rapid increase in the gain (25). Thus, for $\lambda_2 = 22$ μm and $q = 12$, its maximum value [achieved for $x \simeq 1.2$ cm, $\rho_3 \simeq 5 \times 10^{10}$ cm^{-2} and $|\mathcal{E}_1(0)/\mathcal{E}_{1s}(0)| \simeq 1.5$] becomes equal to ~ 10 (Fig. 5), and therefore the corresponding peak power of the 0.1-W input IR pulse achieves ~ 10 W at the point $x \simeq 1.2$ cm, which coincides by the order of magnitude with the optical pulse power for the same x. This means that for large q, the analysis performed above, which neglects the depletion of optical pumping due to its conversion to the IR signal is no longer valid. Nevertheless, we can assert that for $q \gtrsim 12$ and the ~ 0.1-W input IR signal, IR pulses can be amplified up to peak powers of the order of a few tens of watts. Note also that the optimal values of ρ_3 and $|\mathcal{E}_1(0)/\mathcal{E}_{1s}(0)|$ for $\lambda_2 = 22$ and 60 μm (see below) found from numerical simulations differ from the predicted values because the latter were determined qualitatively.

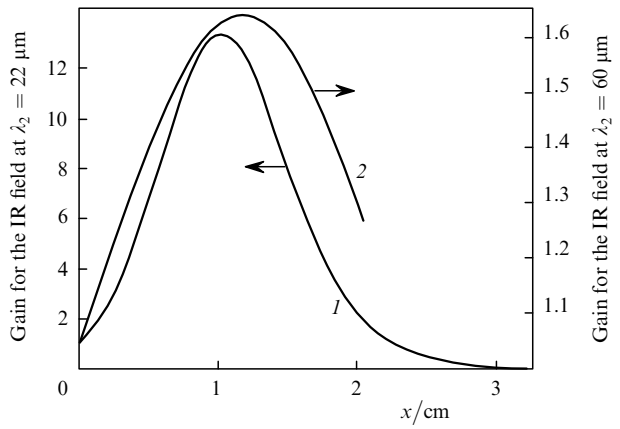

Figure 5. Gain of the IR signal (25) for $\lambda_2 = 22$ μm (*1*) and $\lambda_2 = 60$ μm (2) and parameters indicated in the text.

For $\lambda_2 = 60$ μm, the gain (25) also rapidly increases when the number q exceeds its threshold value ~ 67. Thus, for $q = 100$, $x \simeq 1.2$ cm, $\rho_3 \simeq 7.4 \times 10^9$ cm^{-2} and $|\mathcal{E}_1(0)/\mathcal{E}_{1s}(0)| \simeq 1.3$, it achieves its maximum value 1.6 (the IR signal power increases by more than 2.5 times, Fig. 5). As q further increases, the output IR pulse power increases, of course; however, the transverse dimensions of the active region become greater than the inhomogeneity scale of the optical mode. As a result, the optical field of the optical pulse in many QWs deviates considerably from its optimal value and the rate of increase in the gain with increasing q slows down. Thus, the estimates show that, for example, for $q \sim 300$ the IR power can be increased only by a factor of four.

4. Conclusions

Note that the amplification of the IR pulse can be further increased by placing several heterostructures into the IR beam and introducing optical pulses into each of them at the instants of the IR signal arrival into them (or, similarly to the scheme of synchronously pumped dye lasers [6], by placing a heterostructure into the resonator in which the single-pass transit time of the IR pulse is equal to the repetition period of optical pulses coupled into the resonator through both output mirrors), which solves the problem of the optical pumping depletion. By using the estimates obtained above, we see that for $\lambda_2 = 60$ μm, the IR signal power can be amplified by two orders of magnitude already for five such cascades, each of them containing about 100 QWs (or for five single-pass transits in the resonator).

Being efficient even at room temperature and, therefore, simple for practical applications, the scheme of the amplifier for mid- and far-IR pulses proposed in the paper can be used in medicine for therapy and diagnostics and also for fundamental studies.

Acknowledgements. This work was supported by the Russian Foundation for Basic Research (Grant No. 07-02-00486) and Grant No. NSh4485.2008.2 of the President of the Russian Federation for the State Support of Leading Scientific Schools.

References

1. Faist J., Capasso F., Sivco D.L., Sirtori C., Hutchinson A.L., Cho A.Y. *Science*, **264**, 553 (1994).
2. Hartig M., Ganiere J.D., Selbmann P.E., Deveaud B., Rota L. *Phys. Rev. B*, **60**, 1500 (1999).
3. Tatham M.C., Ryan J.F., Foxon C.T. *Phys. Rev. Lett.*, **63**, 1637 (1989).
4. Vorobjev L.E., Panevin V.Yu., Fedosov N.K., Firsov D.A., Shalygin V.A., Seilmeier A., Schmidt S.R., Zibik E.A., Towe E., Kapaev V.V. *Semicond. Sci. Technol.*, **21**, 1267 (2006).
5. Unuma T., Yoshita M., Noda T., Sakaki H., Akiyama H. *J. Appl. Phys.*, **93**, 1586 (2003).
6. Nekhaenko V.A., Pershin S.M., Poshivalov A.A. *Kvantovaya Elektron.*, **13**, 453 (1986) [*Sov. J. Quantum Electron.*, **16**, 299 (1986)].
7. Basiev T.T., Lokhnygin V.D., Mirov S.B., et al. in *Materialy IV Vsesoyuznoi konferentsii 'Perestraivaemye po chastote lazery'* (Proceedings of the IV All-Union Conference on Tunable Lasers) (Novosibirsk, 1983) p. 399.
8. Arkhangel'skaya V.A., Feofilov P.P. *Kvantovaya Elektron.*, **7**, 1141 (1980) [*Sov. J. Quantum Electron.*, **10**, 657 (1980)].
9. Akhmanov S.A., Vysloukh V.A., Chirkin A.S. *Optics of Femtosecond Laser Pulses* (New York: AIP, 1992; Moscow: Nauka, 1988) p. 248.
10. Sirtori C., Tredicucci A., Capasso F., Fais J., Sivco D.L., Hutchinson A.L., Cho A.Y. *Opt. Lett.*, **23**, 463 (1998).
11. Rochat M., Ajili L., Willenberg H., Faist J., Beere H., Davies G., Linfield E., Ritchie D. *Appl. Phys. Lett.*, **81**, 1381 (2002).
12. Berger V., Sirtori C. *Semicond. Sci. Technol.*, **19**, 964 (2004).
13. Vainshtein L.A. *Elektromagnitnye volny* (Electromagnetic Waves) (Moscow: Sov. Radio, 1988).
14. Chang Y.-C., James R.B. *Phys. Rev. B*, **39**, 12672 (1989).

15. Kapon E. (Ed.) *Semiconductor Lasers* (San Diego: Academic Press, 1999).
16. Madelung O. *Semiconductors: Data Handbook* (Heidelberg, New York: Springer-Verlag, 2003).
17. Altarelli M., Ekenberg U., Fasolino A. *Phys. Rev. B.*, **32**, 5138 (1985).
18. Ekenberg U. *Phys. Rev. B*, **40**, 7714 (1989).
19. Khanin Ya.I. *Osnovy dinamiki lazerov* (Fundamentals of Laser Dynamics) (Moscow: Nauka, 1999).
20. Goodnick S.M., Lugli P. *Phys. Rev. B*, **37**, 2578 (1988).
21. Pikhtin A.N., Yas'kov A.D. *Fiz. Tekh. Poluprovodn.*, **12**, 1047 (1978).
22. Palik E.D., in *Handbook of Optical Constants of Solids*. Ed. by E.D. Palik (New York: Academic, 1985).
23. Gasey N.C. Jr., Panise M.B. *Heterostructure Lasers, Part A* (New York: Academic Press, 1978; Moscow: Mir, Moscow, 1981) Vol. 1.
24. Lockwood D.J., Wasilewski Z.R. *Phys. Rev. B*, **70**, 155202 (2004).
25. Berger V., Sirtori C. *Semicond. Sci. Technol.*, **19**, 964 (2004).
26. Sirtori C., Gmachl C., Capasso F., Fais J., Sivco D.L., Hutchinson A.L., Cho A.Y. *Opt. Lett.*, **23**, 1366 (1998).
27. Delfyett P.J., in *Ultrafast Lasers: Technology and Applications*. Ed. by M.E. Fermann, A. Galvanauskas, G. Sucha (New York, Basel: Marcel Dekker Inc., 2001).